Nonlinear Meissner effect in a *d*-wave superconductor: Extension to all orders of the vector potential

D. Agassi
Functional Materials Department, Naval Surface Warfare Center, Carderock Division, 9500 MacArthur Boulevard, West Bethesda, Maryland 20817-5700, USA

D. E. Oates
MIT Lincoln Laboratory, 244 Wood Street, Lexington, Massachusetts 02420-9108, USA

(Received 17 January 2006; published 24 July 2006)

The analysis of the intrinsic nonlinear Meissner effect in a *d*-wave superconductor is extended here to include all vector-potential orders. This is a continuation of the previously published analysis [D. Agassi and D. E. Oates, Phys Rev. B **72**, 014538 (2005)] that was carried out to third order of the vector potential. The extended analysis now agrees qualitatively with the experimentally determined power dependence. This new analysis also predicts the power level at which the nonlinear response changes from an intrinsic pair-breaking nonlinearity to one where possibly vortex motion dominates.

DOI: 10.1103/PhysRevB.74.024517 PACS number(s): 74.25.Nf, 74.20.Rp, 74.72.Bk

I. INTRODUCTION

The nonlinear Meissner effect, as manifested in a current-dependent penetration depth and in intermodulation distortion (IMD) products, has been observed in high-temperature superconductors (HTS) over a wide domain of temperatures, power, and doping levels.[1,2] The effect, first predicted in the seminal work by Yip and Sauls (YS) at $T=0$, has its origin in the correlated structure of the superconductor condensate state.[3] Further theoretical development by Dahm and Scalapino (DS) generalized the YS work to finite temperatures and to include IMD power dependence on the input power.[4] DS start from an expression for the current density in the presence of a slowly oscillating condensate in response to an external electromagnetic field. A different theoretical approach to the nonlinear Meissner effect has been adopted in a previous publication,[5] in which the focus is on the constitutive relation (CR) that relates the current density and vector potential. In this treatment, the classic London theory corresponds to the *linear* term in the CR, while the lowest-order (third) *nonlinear* term yields the nonlinear Meissner effect. While some of the results in Ref. 5 agree well with the corresponding IMD data, the calculated IMD vs power at a fixed temperature, (the slope on a log-log plot) does not. According to Ref. 5, the slope observable is of particular importance due to its dependence exclusively on intrinsic properties, and hence it provides a stringent test of the theory.

The slope discontinuity predicted in Ref. 5 is not present in the IMD data. It was conjectured in Ref. 5 that this slope discontinuity is an artifact of truncating the constitutive relation at the third order. The conjecture is examined here. By extending the CR calculation to include, approximately, all orders in the vector potential, we find that the slope discontinuity disappears as soon as the CR is extended beyond the third order. However, to qualitatively replicate the data all CR orders are needed. This outcome indicates a slow convergence of the CR expansion. Another result of the all-orders CR extension is the establishment of the power range where the intrinsic nonlinear response dominates. The estimated CR convergence range in terms of a dimensionless expansion parameter [Eq. (2.12)] is interpreted to delineate the crossover from an intrinsic pair-breaking nonlinear response to a nonlinear response dominated by vortex motion.

As in Ref. 5, the static CR relating the Cooper-pair current density and the vector potential in momentum space has the form

$$\vec{j}_S(q) = -\frac{c}{4\pi}K(q)\vec{A}(q) = -\frac{c}{4\pi}\left\{\frac{1}{\lambda_0^2} + K_{\mathrm{NL}}(|\vec{A}(q)|^2)\right\}\vec{A}(q). \tag{1.1}$$

In Eq. (1.1) and hereafter the cgs unit system is employed. The $\vec{j}_S(q)$ and $\vec{A}(q)$ in Eq. (1.1) denote the Cooper-pair current density and electromagnetic potential associated with the one dimensional momentum q, respectively. The chosen gauge is $\vec{\nabla}\cdot\vec{A}=0$ with $\vec{A}_\perp=0$ on the sample's surface, λ_0 denotes the London penetration depth and $K_{\mathrm{NL}}(|\vec{A}(q)|^2)$ is the CR nonlinear scalar kernel. Within the approximations discussed in Ref. 5 and detailed in Sec. II, it has the series expansion

$$K_{\mathrm{NL}}(|\vec{A}(q)|^2) = a_2|\vec{A}(q)|^2 + a_4|\vec{A}(q)|^4 + a_6|\vec{A}(q)|^6 \ldots, \tag{1.2}$$

where the coefficients in Eq. (1.2) are the object of the calculation. The analysis in Ref. 5 is confined to the $a_2|\vec{A}(q=0)|^2$ term, while the analysis here is extended to all terms in Eq. (1.2); thus we call this the all-orders CR. As shown in Sec. II the series in (1.2) can be summed. This is important for the determination of the CR convergence range, mentioned above. The gauge invariance properties of (1.2) are deferred to the last section of this paper.

The paper is organized as follows: In Sec. II the approach and approximations adopted in Ref. 5 are extended to the entire CR expansion in Eq. (1.2). The inversion of the CR in terms of the current, the identification of the dimensionless CR expansion parameter, comparison with IMD slope data, and discussion are covered in Sec. III. Section IV provides a summary of the main results and outlook. Additional technical details are deferred to the Appendices.

II. CONSTITUTIVE RELATION

The CR is derived in the framework of the weak coupling Green function approach to superconductivity in thermal equilibrium. To establish a baseline for notations and to facilitate an uninterrupted presentation, a few basic equations quoted in Ref. 5 are restated here. Our starting point is the imaginary-time Gorkov equations[6]

$$\begin{pmatrix} -\frac{\hbar\partial}{\partial\tau} - \frac{1}{2m}\left(-i\hbar\vec{\nabla} - \frac{q_S}{c}\vec{A}(x)\right)^2 + \mu & \Delta(\vec{r}) \\ \Delta^*(\vec{r}) & -\frac{\hbar\partial}{\partial\tau} + \frac{1}{2m}\left(i\hbar\vec{\nabla} - \frac{q_S}{c}\vec{A}(x)\right)^2 - \mu \end{pmatrix} \begin{pmatrix} g(x,x') & f(x,x') \\ f^*(x,x') & -g(x',x) \end{pmatrix} = \hbar\delta(x-x')\overleftrightarrow{I}. \tag{2.1}$$

In Eq. (2.1) $x=(\vec{x},\tau)$ denotes the space-time coordinates where τ is the imaginary time in the Matsubara formalism, limited to the domain $0\leqslant\tau\leqslant\beta\hbar$ and $\beta=1/(k_BT)$ with k_B denoting the Bolztmann constant, q_S is the *single*-carrier charge (positive or negative), the chosen vector-potential gauge is $\vec{\nabla}\cdot\vec{A}=0$, μ denotes the chemical potential, $\overleftrightarrow{I}$ is the 2×2 unit matrix, $\Delta(\vec{r})$ is the gap function which is assumed to depend only on the relative two-body coordinate $\vec{r}=\vec{x}-\vec{x}'$, discussed in Appendix A, and the ordinary and extraordinary Green functions are $g(x,x')$ and $f(x,x')$, respectively. The Gorkov equations apply for both *s*-wave and *d*-wave gap symmetries.[7]

As in Ref. 5, it will be assumed that a known phenomenological *d*-wave gap function (with no vector-potential dependence) and a vector potential, which is attenuated over a penetration depth λ_0 in the superconductor bulk, provide good approximations to the corresponding self-consistent quantities. These assumptions still leave open the nontrivial task of solving Eq. (1.1) for the Green function matrix $\hat{G}$. The latter has the formal expansion[5,8]

$$\hat{G} = \hat{G}_0 + \frac{1}{\hbar}\hat{G}_0\hat{W}\hat{G}_0 + \frac{1}{\hbar^2}\hat{G}_0\hat{W}\hat{G}_0\hat{W}\hat{G}_0 + \frac{1}{\hbar^3}\hat{G}_0\hat{W}\hat{G}_0\hat{W}\hat{G}_0\hat{W}\hat{G}_0 + \cdots, \tag{2.2}$$

where $\hat{G}_0$, which denotes the unperturbed Green function (when $\vec{A}=0$), and the coordinate-space diagonal interaction $\hat{W}$ are given by

$$\hat{G} = \begin{pmatrix} g(x,x') & f(x,x') \\ f^*(x,x') & -g(x',x) \end{pmatrix},$$

$$\hat{G}_0 = \begin{pmatrix} g_0(x-x') & f_0(x-x') \\ f_0(x-x') & -g_0(x'-x) \end{pmatrix}, \tag{2.3}$$

$$\hat{W} = \frac{i\hbar q_S}{mc}(\vec{A}\cdot\vec{\nabla})\overleftrightarrow{I} - \frac{q_S^2\vec{A}\cdot\vec{A}}{2mc^2}\begin{pmatrix} 1 & 0 \\ 0 & -1 \end{pmatrix},$$

and the unperturbed Green function entries, i.e., $\{g_0(x-x'), f_0(x-x')\}$, are given in Ref. 5. The CR is obtained from the basic Green function expansion Eqs. (2.2) and (2.3) by insertion into the general many-body current-density expression[8]

$$\vec{j}(x) = 2\left\{\frac{i\hbar q_S}{2m}(\vec{\nabla}_{\vec{r}'} - \vec{\nabla}_{\vec{r}})g(x,x') - \frac{q_S^2}{mc}\vec{A}(x)g(x,x')\right\}_{\substack{\vec{r}'\to\vec{r} \\ \tau'\to\tau+0^+}}. \tag{2.4}$$

As in Ref. 5, to render this scheme tractable, further approximations and arguments must be invoked. These should be considered as part of our approach: (1) Only odd-$\vec{A}$ power terms are retained in expansion (2.2). (2) For a microwave-frequency electromagnetic field it is justified to approximate the vector potential by its static limit, i.e., $\vec{A}(\vec{r},t)\approx\vec{A}(\vec{r})$. (3) The interaction $\hat{W}$ in Eq. (2.3) is approximated by retaining only the gradient term, i.e.,

$$\hat{W} \approx \frac{i\hbar q_S}{mc}(\vec{A}\cdot\vec{\nabla})\overleftrightarrow{I}. \tag{2.5}$$

As outlined in Appendix B, in the context of the integration-decoupling approximation of Ref. 5 and Appendix C, all odd-power terms in expansion (2.2) associated with the $\vec{A}\cdot\vec{A}$-term in the interaction $\hat{W}$, Eq. (2.3), cancel out exactly up to and including the ninth order. While we have no mathematical proof that such cancellations persist to arbitrary order, we conjecture that this is true and assert that approximation Eq. (2.5) for the interaction is an excellent one. (4) Noting that the spatially diagonal Green function $g(x,x)$ in Eq. (2.4) is proportional to the total number of carriers,[6] it follows that all nonlinear terms in the CR are contained in the gradient terms of Eq. (2.4). Inserting expansion Eq. (2.2) in Eq. (2.4) with Eq. (2.5) yields

$$\vec{j}^{(\mathrm{NL})}(\vec{r}) = 2\left\{\frac{i\hbar q_S}{2m}(\vec{\nabla}_{\vec{r}'} - \vec{\nabla}_{\vec{r}})g(x,x')\right\}_{\substack{\vec{r}'\to\vec{r} \\ \tau'\to\tau+0^+}}$$
$$= -2\frac{i\hbar q_S}{m}\frac{1}{\hbar^3}\left(\frac{i\hbar q_S}{mc}\right)^3 \vec{\nabla}_{\vec{r}}\left\{\left\langle x\middle|\hat{G}_0\left((\vec{A}\cdot\vec{\nabla})\overleftrightarrow{I}\hat{G}_0\right)^3\middle|x'\right\rangle_{(1,1)}\right\}_{\substack{\vec{r}'\to\vec{r} \\ \tau'\to\tau+0^+}}$$
$$-2\frac{i\hbar q_S}{m}\frac{1}{\hbar^5}\left(\frac{i\hbar q_S}{mc}\right)^5 \vec{\nabla}_{\vec{r}}\left\{\left\langle x\middle|\hat{G}_0\left((\vec{A}\cdot\vec{\nabla})\overleftrightarrow{I}\hat{G}_0\right)^5\middle|x'\right\rangle_{(1,1)}\right\}_{\substack{\vec{r}'\to\vec{r} \\ \tau'\to\tau+0^+}} - \cdots . \tag{2.6}$$

The (1,1) matrix element in Eq. (2.6) is singled out to conform to the matrix notation in Eq. (2.3).

While the structure of the expansion Eq. (2.6) is evident, simplifications and approximations are necessary to enable its evaluation. The analysis and approximations articulated in Ref. 5 with regard to the third-order term (in $\vec{A}$) in Eq. (2.6) apply to the higher-order terms as well. Further details are deferred to Appendix C. To demonstrate the type of expressions that flow from this consider the third-order and fifth-order terms in expansion (2.6). In the one-dimensional strip geometry defined in Fig. 1 and invoking the chosen gauge $\vec{k}\cdot\vec{A}(\vec{k})=0$, the exact expressions are

$$\vec{j}^{(3)}(q) = \int_{-\infty}^{\infty} dz e^{-iqz}\vec{j}^{(3)}(z)$$
$$= -\frac{2q_S{}^4}{\beta(2\pi)^5 m^4 c^3}\sum_{n=-\infty}^{\infty}\int d\vec{k}_1 dq_1 dq_2 \vec{k}_1(\hat{G}_0(\vec{k}_1,\omega_n)(\vec{A}(\vec{q}_1)\cdot\vec{k}_1)\ \overleftrightarrow{I}$$
$$\times \hat{G}_0(\vec{k}_1-\vec{q}_1,\omega_n)(\vec{A}(\vec{q}_2)\cdot(\vec{k}_1-\vec{q}_1))\overleftrightarrow{I}\hat{G}_0(\vec{k}_1-\vec{q}_1-\vec{q}_2,\omega_n)(\vec{A}(\vec{q}-\vec{q}_1-\vec{q}_2)\cdot(\vec{k}_1-\vec{q}))\overleftrightarrow{I}\hat{G}_0\ (\vec{k}_1-\vec{q},\omega_n))_{(1,1)},$$

$$\vec{j}^{(5)}(q) = \int_{-\infty}^{\infty} dz e^{-iqz}\vec{j}^{(3)}(z)$$
$$= -\frac{2q_S{}^6}{\beta(2\pi)^7 m^4 c^3}\sum_{n=-\infty}^{\infty}\int d\vec{k}_1 dq_1 dq_2 dq_3 dq_4 \vec{k}_1(\hat{G}_0(\vec{k}_1,\omega_n)(\vec{A}(\vec{q}_1)\cdot\vec{k}_1)\ \overleftrightarrow{I}$$
$$\times \hat{G}_0(\vec{k}_1-\vec{q}_1,\omega_n)(\vec{A}(\vec{q}_2)\cdot(\vec{k}_1-\vec{q}_1))\overleftrightarrow{I}\hat{G}_0(\vec{k}_1-\vec{q}_1-\vec{q}_2,\omega_n)(\vec{A}(\vec{q}_3)\cdot(\vec{k}_1-\vec{q}_1-\vec{q}_2))\overleftrightarrow{I}$$
$$\times \hat{G}_0(\vec{k}_1-\vec{q}_1-\vec{q}_2-\vec{q}_3,\omega_n)(\vec{A}(\vec{q}_4)\cdot(\vec{k}_1-\vec{q}_1-\vec{q}_2-\vec{q}_3))\overleftrightarrow{I}$$
$$\times \hat{G}_0(\vec{k}_1-\vec{q}_1-\vec{q}_2-\vec{q}_3-\vec{q}_4,\omega_n)(\vec{A}(\vec{q}-\vec{q}_1-\vec{q}_2-\vec{q}_3-\vec{q}_4)\cdot(\vec{k}_1-\vec{q}))\overleftrightarrow{I}\hat{G}_0\ (\vec{k}_1-\vec{q},\omega_n))_{(1,1)}, \tag{2.7}$$

where $\hat{G}_0(\vec{k}_1,\omega_n)$, $\vec{A}(\vec{q}_1)$ are the momentum-space Green function and vector potentials,[5] $\omega_n=(2n+1)\pi/(\beta\hbar)$ are the Matsubara frequencies, and $\vec{j}^{(n)}$ denotes the current density associated with the nth-order term in expansion (2.6). The seemingly complex expressions in Eq. (2.7) have a straightforward meaning in terms of corresponding Feynman diagrams,[5] where each vertex represents a three-momentum-conserving interaction, given in Eq. (2.5), and propagation between vertices is represented by the $\hat{G}_0(\vec{k}_1,\omega_n)$ factors.

Expressions (2.7) are simplified considerably by adopting two approximations, i.e., the decoupling of the q and the $\vec{k}_1$ integrations, and subsequently an approximate q integration. These steps, which were justified and employed in Ref. 5, are extended in Appendix C to the higher-order terms in expansion (2.6). As a result, the leading three nonlinear terms in expansion (2.6) have the approximated expressions,

$$\vec{j}^{(3)}(q) = -\frac{2q_q^4\alpha^{(3)}(q)}{\beta(2\pi)^5 m^4 c^3 \lambda_0^2}\sum_{n=-\infty}^{\infty}\int d\vec{k}_1 \vec{k}_1(\vec{A}(\vec{q})\cdot\vec{k}_1)^2$$
$$\times(\vec{A}(-\vec{q})\cdot\vec{k}_1)((\hat{G}_0(\vec{k}_1,\omega_n))^4)_{(1,1)},$$

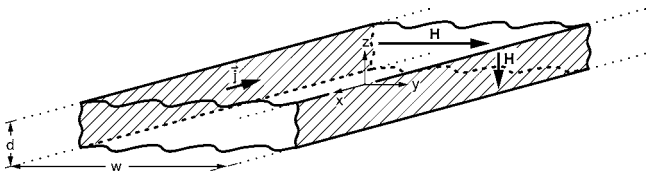

FIG. 1. Schematic current and magnetic field flows pertaining to an infinite superconductor strip, the chosen coordinate system, and the parameters specifying the strip width and thickness.

$$\vec{j}^{(5)}(q) = -\frac{2q_q^6\alpha^{(5)}(q)}{\beta(2\pi)^7 m^6 c^5 \lambda_0^4} \sum_{n=-\infty}^{\infty} \int d\vec{k}_1 \vec{k}_1 (\vec{A}(\vec{q})\cdot\vec{k}_1)^3 \times (\vec{A}(-\vec{q})\cdot\vec{k}_1)^2 ((\hat{G}_0(\vec{k}_1,\omega_n))^6)_{(1,1)},$$

$$\vec{j}^{(7)}(q) = -\frac{2q_q^8\alpha^{(7)}(q)}{\beta(2\pi)^9 m^8 c^7 \lambda_0^6} \sum_{n=-\infty}^{\infty} \int d\vec{k}_1 \vec{k}_1 (\vec{A}(\vec{q})\cdot\vec{k}_1)^4 \times (\vec{A}(-\vec{q})\cdot\vec{k}_1)^3 ((\hat{G}_0(\vec{k}_1,\omega_n))^8)_{(1,1)}. \quad (2.8)$$

The first term in Eq. (2.8) is precisely that discussed in Ref. 5. The dimensionless form factors $\alpha^{(n)}(q)$, which originate from the approximate q integrations in Eq. (2.7), are given in Eq. (C5) for two plausible form factors, i.e., Lorentzian and Gaussian form factors.

The sample of terms in Eq. (2.8) clearly exposes a structure of the entire series of $\vec{j}^{(n)}$ terms. Inserting these in Eq. (2.6) yields for the CR expansion,

$$\begin{aligned}\vec{j}_{\mathrm{NL}}(q) = &-\frac{2q_S^4\alpha^{(3)}(q)}{\beta(2\pi)^5 m^4 c^3 \lambda_0^2} \\ &\times \sum_{n=-\infty}^{\infty} \int d\vec{k}_1 \vec{k}_1 (\vec{A}(\vec{q})\cdot\vec{k}_1)^2 (\vec{A}(-\vec{q})\cdot\vec{k}_1) \\ &\times \left\{ (\hat{G}_0(\vec{k}_1,\omega_n))^4 \times \left(\overleftrightarrow{I} + \left(\frac{q_S}{mc}\right)^2 \frac{1}{(2\pi\lambda_0)^2} \right.\right. \\ &\times \frac{\alpha^{(5)}(q)}{\alpha^{(3)}(q)} (\vec{A}(\vec{q})\cdot\vec{k}_1)(\vec{A}(-\vec{q})\cdot\vec{k}_1)(\hat{G}_0(\vec{k}_1,\omega_n))^2 \\ &+ \left(\frac{q_S}{mc}\right)^4 \frac{1}{(2\pi\lambda_0)^4} \frac{\alpha^{(7)}(q)}{\alpha^{(3)}(q)} (\vec{A}(\vec{q})\cdot\vec{k}_1)^2 \\ &\left.\left. \times (\vec{A}(-\vec{q})\cdot\vec{k}_1)^2 (\hat{G}_0(\vec{k}_1,\omega_n))^4 + \cdots \right) \right\}_{(1,1)}. \quad (2.9)\end{aligned}$$

The bracketed series in the integrand of Eq. (2.9) is *not* a (matrix) geometric series due to the form-factors ratios $\alpha^{(2n+3)}(q)/\alpha^{(3)}(q) \neq 1$; see Eq. (C5). As the plots of $\alpha^{(2n+3)}(q)$ in Fig. 2 show, in the relevant momentum range $|q\lambda_0| \leqslant 1$ the variations of the ratios of form factors are weak and hence are approximated here by their long-wavelength limits $\alpha^{(2n+3)}(0)/\alpha^{(3)}(0)$. Furthermore, we adopt the Lorentzian form factor of Appendix C for these ratios, motivated by the known exponential magnetic field attenuation inside an infinitely thick flat superconducting slab.[9] Accordingly, the

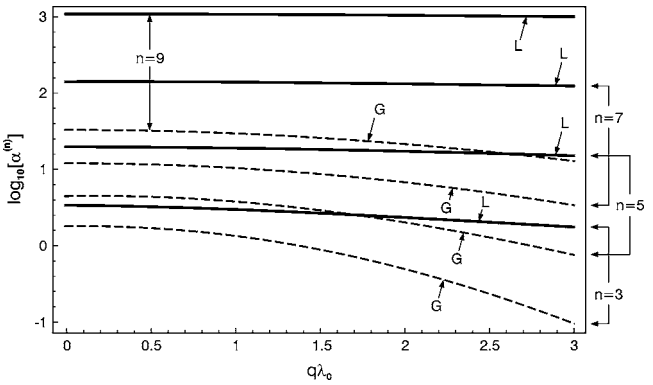

FIG. 2. The factors $\alpha^{(n)}(q\lambda_0)$, Eq. (C5), as a function of $q\lambda_0$ in the range $q\lambda_0 \leqslant 2$ and for $3 \leqslant n \leqslant 9$. The labels L and solid lines, and the label G and broken lines refer to the Lorentzian and Gaussian form factors, respectively, Eq. (C3).

series of form-factor ratios in the bracketed series of the integrand of Eq. (2.9) is

$$\left\{\frac{\alpha^{(2n+3)}(0)}{\alpha^{(3)}(0)}\right\} = \left\{1, \frac{3\pi^2}{5}, \frac{3\pi^4}{7}, \frac{3\pi^6}{9}, \cdots\right\}, \quad (2.10)$$

and consequently the *structure* of the matrix series in the integrand of (2.9) is

$$S(z) = 3\sum_0^{\infty} \frac{z^n}{2n+3} = 1 + \frac{3z}{5} + \frac{3z^2}{7} + \frac{z^3}{3} + \cdots = 3\frac{(-\sqrt{z} + \operatorname{arctanh}[\sqrt{z}])}{z^{3/2}}. \quad (2.11)$$

The point of considering the representative series (2.11) is to expose two features which recur in the exact summation of the bracketed matrix series of the integrand in (2.9) below, i.e., a logarithmic divergence at $z=1$ associated with the function $\operatorname{arctanh}(z)=(1/2)\ln((1+z)/(1-z))$, and the ever slower convergence of the series as $z \to 1$. The latter feature implies that for large z values, a perturbative approach to the CR series in Eq. (2.9) will fail and it must be summed up to all orders. The physical interpretation of the CR convergence range is discussed in Sec. III.

The summation of the bracketed matrix series of the integrand in Eq. (2.9) and associated approximations are detailed in Appendix D. Two important results ensue. The first is the identification of a dimensionless expansion parameter, which corresponds to the z variable in the representative series Eq. (2.11). In terms of the d-wave gap parameterization adopted here, i.e.,

$$\Delta(\vec{k};T) = \Delta(\theta;T) = \Delta_0(T)\cos(2\theta), \quad (2.12)$$

the expression for the expansion parameter is [see Eq. (D12)]

$$v = v(|A(q=0)|^2, T) = \frac{q_S^2 \mu |A(q=0)|^2}{2mc^2 \lambda_0^2(T)\Delta_0^2(T)}. \quad (2.13)$$

In (2.13) μ denotes the Fermi energy and all temperature dependencies are explicitly displayed. Note that the expansion parameter v depends on both the temperature and $|A(q=0)|^2$ factor. However, the latter depends implicitly on the current density by virtue of the CR, which *is* the relation between the current density and vector potential (see Sec. III). Thus, the expansion parameter v reflects the intertwined roles of temperature and current density in determining the low and high IMD power regimes and IMD slope (see below).

The second result of summation of the matrix series in Eq. (2.9) is an explicit expression for the nonlinear CR kernel, Eq. (1.1),

$$K_{\mathrm{NL}}(|A(q)|^2,T) = \frac{4\alpha^{(3)}(0)q_S^2\mu k_F(\hat{c})}{\pi^4\beta(\hbar c)^2\Delta_0(T)} v \sum_{n=-\infty}^{\infty} \mathfrak{I}(v(|A(q=0)|^2,T);\omega_n), \tag{2.14}$$

where the dimensionless function $\mathfrak{I}(v;\omega_n)$ is given by

$$\mathfrak{I}(v(|A(q=0)|^2,T);\omega_n) = \int_0^{2\pi} d\theta \cos^4\theta \int_{-\infty}^{\infty} d\Xi \left[\left(\frac{3}{2(v\cos^2\theta)^{3/2}} \right) \left(\frac{\operatorname{arctanh}\left(\frac{\sqrt{v\cos^2\theta}}{\sqrt{\Xi^2+\cos^2 2\theta}-i\Omega_n} \right)}{\sqrt{\Xi^2+\cos^2 2\theta}-i\Omega_n} + \text{c.c.} \right) - \frac{3(\Xi^2+\cos^2 2\theta-\Omega_n^2)}{v\cos^2\theta(\Xi^2+\cos^2 2\theta+\Omega_n^2)} \right]. \tag{2.15}$$

The dimensionless variables Ξ, Ω_n in Eq. (2.15) are related to the excitation energy relative to the Fermi energy [Eq. (D5)] and Matsubara frequencies by

$$\Xi = \frac{\xi}{\Delta_0}, \quad \Omega_n = \frac{\hbar\omega_n}{\Delta_0} = \frac{(2n+1)\pi k_B T}{\Delta_0}. \tag{2.16}$$

The all-orders nonlinear CR kernel, Eqs. (2.14)–(2.16), is the central result of this work. All entries in the expression for K_{NL} are available from experimental data. Thus it is a parameter-free expression. Note also the appearance of the arctanh[z] function, in analogy to the representative series, Eq. (2.11). Since the integrand of (2.15) draws its main contribution from near the Fermi energy, where $\Xi \sim 0$, and from the Matsubara frequencies $n=0,-1$, the integrand tends to diverge logarithmically for $v \sim 1$, in analogy to the exact logarithmic divergence encountered in the representative series (2.11) at $z=1$. These features are further discussed in Sec. III.

A simple check of expressions (2.14) and (2.15) is to consider its $v \to 0$ limit. According to expansion (2.9), the expression for K_{NL} in this limit should coincide with that given in Ref. 5. In the lowest orders, the expansion of the integrand of Eq. (2.15) in v is

$$\mathfrak{I}(v;\omega_n) = \int_0^{2\pi} d\theta \cos^4\theta \int_{-\infty}^{\infty} d\Xi \left[\left(\frac{1}{2(\sqrt{\Xi^2+\cos^2 2\theta}-i\Omega_n)^4} + \text{c.c.} \right) + \left(\frac{3\cos^2\theta}{10(\sqrt{\Xi^2+\cos^2 2\theta}-i\Omega_n)^6} + \text{c.c.} \right) v + O(v^2) \right]. \tag{2.17}$$

The analytic Ξ integration of the v^0 term in (2.17) in combination with the other factors in Eq. (2.9) yields precisely the expression for K_{NL} in Ref. 5. Furthermore, the Ξ integration of the first-order term in v in Eq. (2.17) (involving the $\hat{G}_0{}^6$ factor) has been checked to be identical to the corresponding term in Eq. (2.9). An additional check is carried out in Appendix D. These checks substantiate the veracity of expression (2.15).

To complement the consideration of the $\lim_{v\to 0} \mathfrak{I}(v;\omega_n)$ above and for the considerations in the next section, consider now the $v \to \infty$ limit Eq. (2.15). The result is

$$\mathfrak{I}(v;\omega_n) = \int_0^{2\pi} d\theta \cos^4\theta \int_{-\infty}^{\infty} d\Xi \left(-\frac{3(1+2\Xi^2-2\Omega^2+\cos(4\theta))}{\cos^2\theta(\Xi^2+\Omega^2+\cos^2(2\theta))^2} \times \frac{1}{v} + O(v^{-2}) \right), \tag{2.18}$$

indicating that $\mathfrak{I}(v;\omega_n)$ is always negative and tends to zero from below for arbitrarily large values of the v parameter. The expectation that the nonlinear kernel K_{NL} is always negative is implied by the CR, Eq. (1.1), since the nonlinear pair-breaking processes are expected to weaken superconductivity and hence to increase the effective penetration depth.

III. RESULTS AND DISCUSSION

As was mentioned in the Introduction, the primary motivation for the extension of the calculation of the CR to all orders in the vector potential is the determination of the IMD on the circulating power. This calculation is presented below. The consideration of the all-orders CR also sheds light on the issue of the power domain where intrinsic nonlinearity is expected to dominate. The procedure here follows the slope calculation procedure in Ref. 5.

Taking the absolute square of the CR, Eq. (1.1), expressing the nonlinear kernel in terms of dimensionless quantities, Eq. (2.14), and expressing the momentum-space current density in terms of the total current I in the strip geometry[5]

$$j(q=0)=\frac{I}{d}, \tag{3.1}$$

yields the implicit equation for the expansion parameter v, Eq. (2.13), in terms of the total current

$$\frac{8\pi^2\lambda_0^2\mu q_S^2 I_{\mathrm{REF}}^2}{m_{ab}c^4\Delta_0^2 d^2}\left(\frac{I}{I_{\mathrm{REF}}}\right)^2 = v\left(1+\frac{4\alpha^{(3)}q_S^2 k_F(\hat{c})\mu\lambda_0^2}{\pi^4\beta(\hbar c)^2\Delta_0}v\sum_{n=-\infty}^{\infty}\mathfrak{I}(v;\omega_n)\right)^2. \tag{3.2}$$

In Eq. (3.2) I_{REF} denotes a reference current chosen below, and the explicit temperature dependencies have been suppressed for the sake of notational simplicity. The procedure then is to solve Eq. (3.2) for $v(I^2,T)$, insert that solution in the expression for the nonlinear kernel, Eqs. (2.14) and (2.15), and from that calculate the dependence of the IMD power on the circulating power, following the procedure outlined in Ref. 5. When the IMD power versus circulating power is displayed on a double logarithmic plot, the dependence is seen as the slope of the curve, yielding the power law of the dependence. We proceed first with the discussion of Eq. (3.2) employing the all-orders expression for $\mathfrak{I}(v,\omega_n)$, Eqs. (2.14) and (2.15). Finite-order approximations (in v) are examined subsequently.

The parameters employed in Eq. (3.2) are those employed in Ref. 5, recapped here for the sake of self-containment. The strip width and thickness of the resonator are $w=150$ μm and $d=0.35$ μm, respectively. The gap function parameter and linear penetration depth are $\Delta_0(T=0)=0.024$ eV,[10] and $\lambda_0(T=0)=0.2$ μm.[1] The measured samples are overdoped $YBa_2Cu_3O_{7-\delta}$ with an estimated 0.34 holes/unit cell. Given the unit cell volume $(a_a)^2a_c$, where $a_a\approx a_b=0.38$ nm, $a_c=1.17$ nm, this doping level transcribes to a hole density $n=1.7\times10^{21}$ cm^{-3}. The effective mass, identified with the effective ab-plane mass, can be estimated either from the measured bulk plasma frequency $(\hbar\omega_P)^2=4\pi e^2 n(\hbar c)^2/(m^*c^2)$ or the penetration depth $\lambda_0^2=m^*c^2/(4\pi e^2 n)$ (Ref. 9) by inserting the above-estimated hole density. However, these two effective mass estimates are not identical. As a compromise we adopt the value $m^*/m_0=2$ (where m_0 is the rest mass of the electron) which yields $\lambda_0(T=0)\simeq 182$ nm and $\hbar\omega_P\simeq 1.1$ eV, in good agreement with experimental numbers $\lambda_0(T=0)=200$ nm and $\hbar\omega_P\simeq 1.4$ eV.[11] The ensuing Fermi energy is $\mu\simeq 0.3$ eV and the c axis Fermi momentum is taken as $k_F(\hat{c})=\pi/a_c=3.2$ nm^{-1}. The following discussion pertains to a temperature $T=1.75$ K motivated by the existing data in Ref. 5.

To compare the theoretical predictions with IMD versus power data, we first transcribe power P to dimensionless dBm units, defined as

$$P(\text{in dBm})\equiv 10\log_{10}\left(\frac{P}{1\ \text{mW}}\right). \tag{3.3}$$

The circulating power in the strip is given by $P_{\mathrm{CIRC}}=I^2Z_0$, where Z_0 denotes the resonator characteristic impedance. This suggests a circulating power variable x (in dBm units) defined as

$$x=10\log_{10}\left(\frac{P_{\mathrm{CIRC}}}{1\ \text{mW}}\right)=10\log_{10}\left(\frac{I}{I_{\mathrm{REF}}}\right)^2\Rightarrow\left(\frac{I}{I_{\mathrm{REF}}}\right)^2=10^{x/10}, \tag{3.4}$$

where the reference current in (3.4) is chosen for convenience so that $I_{\mathrm{REF}}^2Z_0=1$ mW. Given the resonator's characteristic impedance of $Z_0=33$ Ω, the corresponding reference current is $I_{\mathrm{REF}}=5.5\times10^{-3}$A. Consequently, expressing the left-hand side of Eq. (3.2) in terms of the variable x in (3.4), the solution of Eq. (3.2) is $v(x,T)$. With these preparatory remarks, and according to Ref. 5, the IMD power P_{IMD} is given by

$$P_{\mathrm{IMD}}(I,T)=C(T)\left(\frac{I}{I_{\mathrm{REF}}}\right)^2K_{\mathrm{NL}}^2(v(x),T), \tag{3.5}$$

where $C(T)$ represents all current-independent factors, such as I_{REF}^2. Consequently, the IMD power and the slope of P_{IMD} vs P_{CIRC} on a double logarithmic plot, denoted by $y(x)$ and dy/dx, respectively, are given in dBm by

$$y(x)=P_{\mathrm{IMD}}(\text{in dBm})=10\log_{10}C_1(T)+x+20\log_{10}\left(v\left|\sum_{n=-\infty}^{\infty}\mathfrak{I}(v(x),\omega_n;T)\right|\right), \tag{3.6}$$

$$\frac{dy}{dx}=1+20\frac{d}{dx}\left(\log_{10}\left(v\left|\sum_{n=-\infty}^{\infty}\mathfrak{I}(v(x),\omega_n;T)\right|\right)\right),$$

where the current-independent factor $C_1(T)$ is associated with the factor $C(T)$ in Eq. (3.5) and current-independent factors in Eq. (2.14). Note that for a fixed temperature the slope in Eq. (3.6) has no adjustable parameters.

For the inversion Eq. (3.2) in order to obtain $v(x,T)$, it is depicted in Fig. 3. Figure 3(a) shows the function $K_{\mathrm{NL}}(v)/v$, which according to Eq. (2.14) is the product of the dimen-

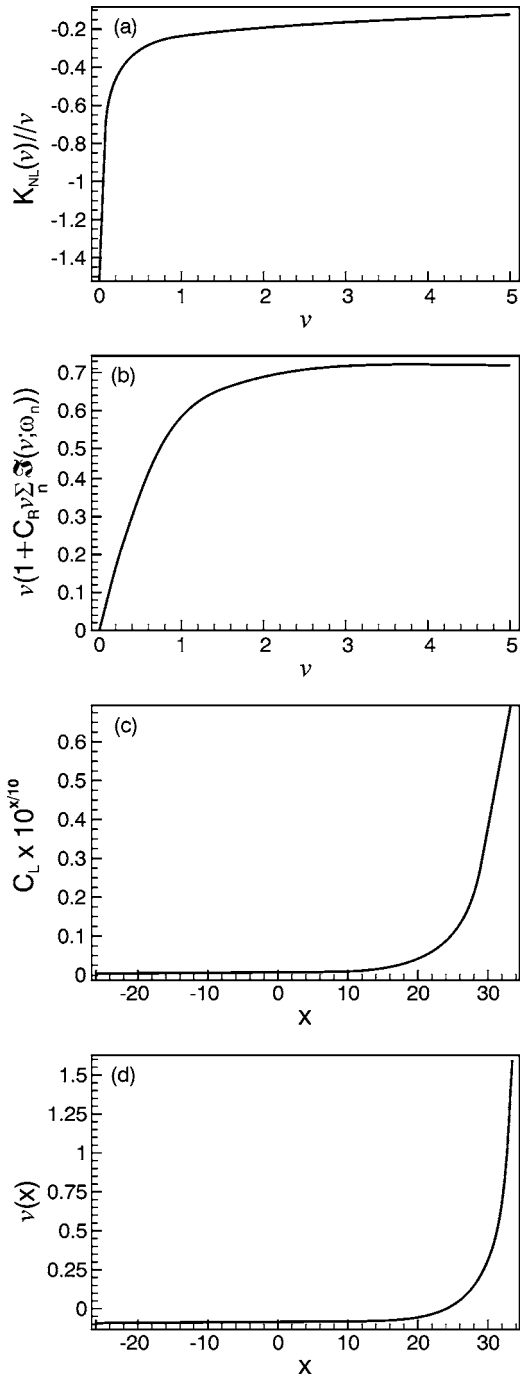

FIG. 3. Intermediate steps in the inversion of the squared-CR, Eq. (3.2), for the expansion parameter v, Eq. (2.13) at $T=1.75$ K. The circulating power variable x is defined in Eq. (3.4). (a) The nonlinear kernel, Eq. (2.14). (b) The right-hand side of Eq. (3.2). (c) The left-hand side of Eq. (3.2). (d) The solution of inverting Eq. (3.2), $v(x)=v(x,T=1.75\ \mathrm{K})$. Further discussion is detailed in Sec. III.

sionless function $\Im(v;\omega_n)$ summed over all Matsubara frequencies ω_n and the appropriate v-independent prefactors. This function is always negative, since the nonlinear contributions *increase* the penetration length; see the CR, Eq. (1.1). The corresponding Taylor expansions in v and v^{-1}, given in Eqs. (2.17) and (2.18), confirm this explicitly. The curve in Fig. 3(a) exhibits a characteristically large slope and values for $v \leqslant 0.6$ followed by a smooth transition to a small slope and values for $v > 0.6$. Like in the representative series Eq. (2.11), at the source of this characteristic is the arctan $h(x)$ function in Eq. (2.15) which starts at a zero value for $x=0$, diverges logarithmically at $x=1$ and at $x \to \infty$ tends to $i\pi/2$. An imaginary argument in the arctan $h(x)$ function, as in Eq. (2.15), transforms the logarithmic divergence into a maximum which strongly impacts the value of the integral. To see this, note that the integrand in (2.15) draws its main contribution from near $\Xi \approx 0$ and the normalized Matsubara frequencies $\Omega_{-1}=-\Omega_0$. There the arctan $h(x)$ function in Eq. (2.15) has the approximate argument

$$\frac{\mathrm{arctanh}\left(\frac{\sqrt{v\cos^2\theta}}{\sqrt{\Xi^2+\cos^2 2\theta}-i\Omega_n}\right)}{\sqrt{\Xi^2+\cos^2 2\theta}-i\Omega_n} \approx \frac{\mathrm{arctanh}\left(\frac{\sqrt{v\cos^2\theta}}{\sqrt{\cos^2 2\theta}-i\Omega_0}\right)}{\sqrt{\cos^2 2\theta}-i\Omega_0}. \tag{3.7}$$

As Eq. (3.7) indicates, the maxima of the integrand arises when $\sqrt{v}\cos(\theta) \approx \cos(2\theta)$ and $\cos(2\theta) \approx 0$. Numerical examination of these conditions shows that for $v \leqslant 0.6$ there are four θ points where they are approximately satisfied, while for $v > 0.6$ only two such θ points exist. The factors $v^{-3/2}, v^{-1}$ in (2.15) further overemphasize the contribution and rapid variation for $v \leqslant 1$; hence the two-slope characteristics exhibited in Fig. 3(a).

Figure 3(b) shows the right-hand side of Eq. (3.2) as a function of v, where all v-independent prefactors are lumped into the constant C_R. The two-slope characteristics and saturation at $v \to \infty$ of $\Sigma_n \Im(v;\omega_n)$ of Fig. 3(a) are reflected here, although smoothed out by the structure of the right-hand side of Eq. (3.2). Note that for $v \gg 1$ values (not shown), the plateau in Fig. 3(b) would end and be replaced by a linear, unrestricted increase (see below). Figure 3(c) shows the left-hand side of Eq. (3.2), where all current-independent prefactors are lumped into the constant C_L. The $(I/I_{\mathrm{REF}})^2$ factor, on the other hand, is expressed as in Eq. (3.4). By comparing it to the right-hand side of Eq. (3.2) in Fig. 3(b) two observations stand out: (a) For circulating-power levels above the threshold of $x_{\mathrm{TH}} \approx 32$ dBm the inverse of Eq. (3.2) does not exist in the domain, $0 \leqslant v \leqslant 5$. Stated differently, for $x > x_{\mathrm{TH}}$ the solution of Eq. (3.2) becomes unstable in the sense that a small change in x implies a disproportionably large change in the corresponding v which is associated with the large-v linear extension of the curve in Fig. 3(b) (not shown; see comment above). This instability is interpreted below to indicate a change in the underlying physics. (b) For a sufficiently small current I, Eq. (3.2) has a solution $[v \propto |\vec{A}|^2 \propto x \propto I^2$; see Eq. (2.13)]. This is just the low-power London limit where $\vec{j} \propto \vec{A}$,[9] as expected. As the relative current I/I_{REF} increases, the solution of Eq. (3.2), $v(x,T)$, increasingly deviates from its London limit up to the point where an instability is encountered, due to the quasiplateau in Fig. 3(b). The

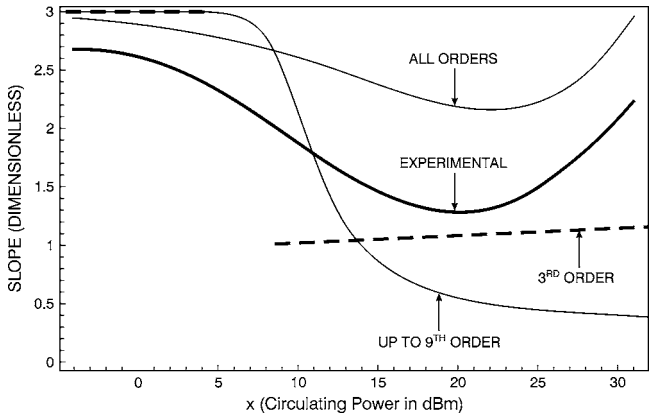

FIG. 4. The calculated IMD power slope versus the circulating power, Eq. (3.6), for several levels of approximations of the CR expansion, Eq. (1.1). The broken line, denoted "3rd ORDER" and adapted from Ref. 5, refers to retaining only the second order in $\vec{A}(q)$ in expansion (1.2). The curve denoted "UP TO 9th ORDER" includes all CR terms in Eq. (1.2) up to the 8th order. The curve denoted "ALL ORDERS" results from considering all orders in Eqs. (1.2) and (3.2). The measured slope, adapted from Ref. 5, is denoted by "EXPERIMENTAL."

solution $v(x)$ to Eq. (3.2) is plotted in Fig. 3(d) for x values up to x_{TH}, where $v(x_{\mathrm{TH}}) \approx 1.5$.

Inserting $v(x,T)$ into the slope expression, Eq. (3.6), yields the calculated all-orders slope plotted in Fig. 4. While not exactly replicating the experimental slope, the calculated curve does not exhibit a discontinuity and captures the main qualitative features of the experimental curve such as an inverted bell-shaped curve, a minimum at approximately the right place where $|x_{\mathrm{MIN}}(\mathrm{exp}) - x_{\mathrm{MIN}}(calc)| \approx 3$ dBm and a slope reasonably close to the data. These results are obtained without adjustable parameters in the calculation.

To put the all-orders curve in Fig. 4 in perspective, it is instructive to compare it to finite-order calculations. This comparison sheds light on the convergence properties of the CR series, Eq. (2.9), and demonstrates the necessity to consider an all-orders calculation. For this purpose we added in Fig. 4 the calculated slopes that result from keeping in expansion Eq. (2.9) only the third-order term (in $\vec{A}$), as in Ref. 5 and the result for all terms up to the ninth order. The series of curves in Fig. 4 clearly support the conjecture that the slope discontinuity encountered in Ref. 5 is indeed associated with the CR truncation at the third order. However, while higher-order CR truncations produce a continuous slope, the initial slope $dy/dx \approx 3$ for $x < 0$ (the London limit) is followed by a *downturn* for higher x values without further upturn. Only the all-orders calculation reproduces the observed slope upturn for higher x values. This situation implies a slow or asymptotic convergence of the CR expansion, which necessitates a summation to all orders for reliable results for the slope observable.

We now turn to the discussion on the implications of the circulating-power threshold x_{TH}, Fig. 3, at which the squared CR solution $v(x,T)$ undergoes a sudden change in its functional dependence. This threshold suggests a crossover from intrinsic nonlinearity, which is the focus of this work and Ref. 5, to nonlinearity associated with an extrinsic origin, such as vortex motion in response to the field-induced oscillating currents. The suggestion of the vortex motion as the source of the observed nonlinear response is supported by the following estimates of the associated field and (kinetic) energy at the threshold power level x_{TH}: (a) the current density j_{TH} associated with $v_{\mathrm{TH}} = v(x_{\mathrm{TH}},T)$ is $j_{\mathrm{TH}} = (I_{\mathrm{REF}}/(wd))10^{x_{TH}/20} \approx 4.2 \times 10^5$ A/cm^2. The corresponding peak magnetic field at the strip edges is $H_{\mathrm{TH}} \approx 100$ G,[12] which is of the order of H_{C1} of bulk YBCO samples and definitely larger than that of YBCO thin films.[13] The proximity of the fields $H_{C1} \sim H_{\mathrm{TH}}$ is consistent with an onset of vortex dynamics as the source for the observed nonlinearity. (b) The Lorentz force F_P exerted by a current j on a vortex of length L is $F_P/L = (\Phi_0 j)/c$, Refs. 14 and 15, and the corresponding energy is on the order $E_{\mathrm{TH}} \sim F_P \lambda_0$. Inserting the vortex length the film thickness $L = d = 350$ nm and the threshold current j_{TH} estimate above, yields $E_{\mathrm{TH}} = 3.7$ eV. This characteristic energy should be compared to pinning energies E_P of typical defects, such as grain boundaries and point defects, in order to assess if it is sufficiently large to dislodge vortices from their pinning sites and thereby bringing into play vortex dynamics as a source for a nonlinear response. Consider first low-angle grain boundaries, which are believed to provide the strongest pinning sites. The critical current densities associated with these defects (and twin boundaries) are on the order of 10^7 A/cm^2,[16] considerably higher than j_{TH}. This implies that vortices pinned at these defects are not depinned by a current density on the order of j_{TH}, and hence unlikely to participate. At the opposite extreme are point defects, with a typical pinning temperature of $T_P = 800$ K, or E_P (pd) ~ 0.07 eV,[17] or a distribution of pinning energies.[18] That $E_{\mathrm{TH}} \gg E_p$ (pd) may suggest that vortices pinned to point defects are not associated with an onset of vortex dynamics at current density levels on the order of j_{TH}. This leaves us with vortices pinned to large-angle grain boundaries, which act as Josephson junctions or other depinning scenarios. The nonlinear vortex motion along a long Josephson junction has been considered before.[19,20] However, this model does not account for nonlinear surface impedance data on YBCO films.[18] Another proposed source of vortex-related nonlinearity is the depinning of vortex *segments* by thermal activation between metastable states that are separated by distance on the order of a coherence length.[21] These brief remarks demonstrate that while the proposition of vortex motion as the source of nonlinearity at high power levels is plausible, details of this physical picture remain to be studied.

IV. SUMMARY

We have developed a systematic microscopic framework for calculating the CR to all orders in the vector potential in the static limit. The expansion parameter underlying the CR expansion, Eq. (2.13), has been identified and depends on both the power level (or total current) and the temperature [Eq. (3.2)]. This former dependence leads to prediction of a maximum power level (at a given temperature) for which intrinsic nonlinearity applies. Above that power level maxi-

mum we expect a crossover to a regime where nonlinearity is dominated by extrinsic effects such as motion of depinned vortices.

The all-orders CR is employed here for the calculation of the IMD power versus the circulating power slope on a log-log plot. This observable depends only on intrinsic properties such as the gap and penetration depth. In a previous work[5] this slope calculation has been attempted employing, however, the CR to third order only. The corresponding calculations agreed poorly with the data of high-quality YBCO films.[1] Given that the present CR extension does not employ adjustable parameters, the IMD slope calculation is in good qualitative agreement with the same data. The slow convergence of the CR expansion, as manifested by results of finite-order CR truncation approximations, mandates consideration of the CR to all orders as we did here. The remaining differences between the data and the calculation, Fig. 4, may be attributed to several factors such as the accuracy of basic approximations, the integration-decoupling approximation of Sec. II, the static approximation or the effect of impurity scattering. Future studies are needed to clarify these issues.

With regard to the issue of the CR gauge invariance we can offer extension of arguments employed in discussing the London (linear) CR. The results of the starting Gorkov equations, Eq. (2.1), are gauge invariant.[22] In our chosen gauge ($\vec{\nabla}\cdot\vec{A}=0, \vec{A}_{\perp}=0$ on the strip surface) and the geometry of Fig. 1, linear terms in the CR are gauge invariant for the single-connected body.[23] For the CR nonlinear terms in the static limit we have $\vec{A}(\vec{q})\cdot\vec{A}(\vec{q}) \Rightarrow \vec{A}'(\vec{q})\cdot\vec{A}'(\vec{q})=\vec{A}(\vec{q})\cdot\vec{A}(\vec{q}) - (\vec{q}\cdot\vec{q})\Lambda(\vec{q})^2$, where $\Lambda(\vec{q})$ is an arbitrary gauge function and $\vec{q}=(0,0,q_Z)$[24]. Hence in the long-wavelength limit ($q\to 0$) all terms in Eq. (1.1) do not depend on the arbitrary gauge function. The latter is the limit corresponding to the measurements and discussed in this work.

The calculation of the nonlinear response of a superconductor in the strong electron-phonon coupling regime has been recently reported.[25] Unlike the calculation in this work, the former is fully self-consistent and yields, in particular, the gap renormalization due to the circulating current. The reported effects, however, are small in comparison to the overall observed IMD power variation (see Ref. 5, and references therein), in particular at the low temperature considered in this work.

ACKNOWLEDGMENTS

The work at Lincoln Laboratory was supported by the Air Force Office of Scientific Research. The work at NSWC was supported by the Naval Surface Warfare Center ILIR program.

APPENDIX A: THE GORKOV EQUATIONS, EQ. (2.1)

The Gorkov equations for an arbitrary-symmetry gap have the form[26]

$$\left\{ i\hbar\omega_n - \frac{1}{2m}\left(-i\hbar\vec{\nabla}_{\vec{x}} - \frac{q_S}{c}\vec{A}(\vec{x})\right)^2 + \mu \right\} g(\vec{x},\vec{x}';\omega_n) + \int d\vec{x}''\Delta(\vec{x},\vec{x}'')f(\vec{x}'',\vec{x}';\omega_n) = \hbar\delta(\vec{x}-\vec{x}'), \tag{A1}$$

where $\Delta(\vec{x},\vec{x}')$ denotes the nonlocal gap function. The issue is under which conditions the nondiagonal term in Eq. (A1) can be approximated by a product, as in Eq. (2.1).

Consider the following two-particle relative and center-of-mass coordinates:

$$\vec{r}''=\vec{x}-\vec{x}'', \quad \vec{r}'=\vec{x}''-\vec{x}', \quad \vec{r}=\vec{x}-\vec{x}',$$

$$\vec{R}''=\frac{\vec{x}+\vec{x}''}{2}, \quad \vec{R}'=\frac{\vec{x}''+\vec{x}'}{2}, \quad \vec{R}=\frac{\vec{x}+\vec{x}'}{2}. \tag{A2}$$

As a function of the two-body relative coordinate, the gap and Green function in the nondiagonal term in Eq. (A1) decay over a coherence length ξ.[7] Thus $|\vec{r}'|\sim|\vec{r}''|=O(\xi)\Rightarrow|\vec{r}|=O(\xi)$, and in particular $|\vec{R}'-\vec{R}|=|\vec{x}-\vec{x}''/2|=O(\xi)$. Therefore, for the Green function for instance,

$$\begin{aligned} f(\vec{x}'',\vec{x}';\omega_n) &= f(\vec{R}',\vec{r}';\omega_n) \\ &= f(\vec{R},\vec{r}';\omega_n)\{1+(\vec{R}'-\vec{R}) \\ &\quad \cdot(\vec{\nabla}_R f(\vec{R},\vec{r}';\omega_n))/f(\vec{R},\vec{r}';\omega_n)+\cdots\} \\ &= f(\vec{R},\vec{r}';\omega_n)\{1+O(\xi/\lambda)\}\approx f(\vec{R},\vec{r};\omega_n). \end{aligned} \tag{A3}$$

In passing from the second to the third line in (A3) it has been assumed that the Green-function $\vec{R}$ variation tracks that of the vector potential (otherwise, in a homogeneous superconductor there would be no $\vec{R}$ variation), i.e.,

$$\left|\frac{\vec{\nabla}_R f(\vec{R},\vec{r}';\omega_n)}{f(\vec{R},\vec{r}';\omega_n)}\right| = O(\lambda^{-1}), \tag{A4}$$

$|\vec{r}'|\sim|\vec{r}|=O(\xi)$ and that $\xi/\lambda\ll 1$. These approximations, and limiting the x'' integration in Eq. (A1) such that $|\vec{r}'|=O(\xi)$ yield for the nondiagonal term in Eq. (A1) a product form.

APPENDIX B: THE CONTRIBUTIONS OF THE $(\vec{A}\cdot\vec{A})$ TERM IN EQ. (2.3) TO THE CR

In the context of the Green-function expansion to all orders [Eq. (2.2)], the contributions of terms which involve the $(\vec{A}\cdot\vec{A})$ interaction in Eq. (2.3) must be examined since *mixed* terms, which include both the gradient-interaction term, Eq. (2.5), and $(\vec{A}\cdot\vec{A})$-interaction term, constitute the majority of the terms.

In the third order, estimates in Ref. 5 of single $(\vec{A}\cdot\vec{A})$ and $(\vec{\nabla}\cdot\vec{A})$ terms were found to be comparable. It was argued there that a factor on the order of 2 is not critical, hence only the gradient-interaction term was kept. In the present context of considering all odd-$\vec{A}$ orders in (2.2), this argument is clearly invalid. The calculations outlined below demonstrate that within the integration-decoupling approximations that led to expressions Eq. (2.8), all odd-$\vec{A}$-order contributions to expansion (2.2) which involve the $(\vec{A}\cdot\vec{A})$-interaction term cancel out exactly, up to and including the *ninth* order in the

vector potential. We consider this result a sufficient indication that all terms involving the $(\vec{A}\cdot\vec{A})$ interaction cancel out in the context of the approximations adopted here. Consequently, the gradient term, Eq. (2.5), provides an excellent approximation to the interaction.

Consider first the third-order (in $\vec{A}$) contributions. Since only odd-$\vec{A}$ powers are relevant, there are only two terms in expansion (2.2) in this order which involve the $(\vec{A}\cdot\vec{A})$ interaction. Under our integration-decoupling approximations (Appendix C) for the one-dimensional geometry of Fig. 1 and in terms of the expressions

$$\vec{A}(\vec{r}) = \frac{1}{2\pi}\int d\vec{q}e^{i\vec{q}\cdot\vec{r}}\vec{A}(\vec{q}), \quad \vec{A}(\vec{q}) = (A_x(q_z),0,0)\delta(q_x)\delta(q_y),$$

$$\vec{j}(z) = \frac{1}{2\pi}\int dq_z e^{iq_z z}\vec{j}(q_z), \quad \vec{j}(q_z) = (j_x(q_z),0,0), \quad \text{(B1)}$$

one of the two terms has the expression

$$j^{(3)}_{(\vec{A}\cdot\vec{A})(\nabla\cdot\vec{A})}(q) = \frac{q_S^4\gamma^{(3)}}{2(2\pi)^4 m^3 c^3 \beta\hbar\lambda_0}A^{(2)}(0) \times \sum_{n=-\infty}^{\infty}\int d\vec{k}_1\vec{k}_1(\vec{A}(q)\cdot\vec{k}_1) * \{\hat{m}\hat{\tau}_Z\hat{m}\vec{\vec{I}}\hat{m}\}_{(1,1)}. \quad \text{(B2)}$$

The new symbols in Eq. (B1) are defined by

$$\hat{m} = \hat{G}_0(k_1) = \begin{pmatrix} g_0(\xi(k)) & f_0(\xi(k)) \\ f_0(\xi(k)) & -g_0^*(\xi(k)) \end{pmatrix},$$

$$\hat{\tau}_Z = \begin{pmatrix} 1 & 0 \\ 0 & -1 \end{pmatrix}, \quad A^{(2)}(0) = 2\pi\int_{-\infty}^{\infty} dq|A(q)|^2. \quad \text{(B3)}$$

The constant $\gamma^{(3)}$ is an uninteresting dimensionless number associated with an approximate q integration, analogous to the $\alpha^{(n)}$ in Eq. (2.8), ξ is the relative energy (with respect to the Fermi level; see Ref. 5 Appendix A), and the ω_n dependencies in $\{g_0,f_0\}$ are suppressed.

In addition to the term in Eq. (B3) there is a twin term where the places of the $(\vec{A}\cdot\vec{A})$ and $(\vec{\nabla}\cdot\vec{A})$ factors are interchanged. The prefactors and angular integrations in both terms are the same. After replacing the $\vec{k}_1$ integrations in (B3) and its twin term into angular and ξ variables, as in Ref. 5, the two terms differ by only the factors which involve the Green function factors and ξ integration. These are explicitly given next and calculated to yield

$$\int_{-\infty}^{\infty} d\xi\{m\cdot\vec{\vec{I}}\cdot m\cdot\hat{\tau}_Z\cdot m\}_{(1,1)} = \int_{-\infty}^{\infty} d\xi\{m\cdot\hat{\tau}_Z\cdot m\cdot\vec{\vec{I}}\cdot m\}_{(1,1)} = 0. \quad \text{(B4)}$$

Hence, in the third order (in $\vec{A}$) the $(\vec{A}\cdot\vec{A})$ terms are justifiably ignored. This short exercise points out the way to quickly assess higher-order terms by considering just the factors involving Green functions and the associated ξ integration, as in Eq. (B4), noting that all other factors in the complete expressions of the pertinent terms are the same. With this insight, consider now the fifth-order terms.

In the fifth order there are seven terms which involve the $(\vec{A}\cdot\vec{A})$ interaction. They are classified according to the power n of the $(\vec{A}\cdot\vec{A})$ interaction in their Green function integrands. Within each of these subgroups, all other integrations and factors are the same; hence they need not be explicitly considered in the present discussion. Obviously, for the fifth order $0<n\leqslant 2$. By inspection, the seven pertinent Green-function integrals are classified according to the order of the $\hat{\tau}_Z$ matrix factor. Explicit calculations yield

$$\hat{\tau}_Z: \int d\xi\{\hat{m}\cdot\tau_Z\cdot\hat{m}\cdot\hat{m}\cdot\hat{m}\cdot\hat{m}\}_{(1,1)} = -\int d\xi\{\hat{m}\cdot\hat{m}\cdot\tau_Z\cdot\hat{m}\cdot\hat{m}\cdot\hat{m}\}_{(1,1)} = -\int d\xi\{\hat{m}\cdot\hat{m}\cdot\hat{m}\cdot\tau_Z\cdot\hat{m}\cdot\hat{m}\}_{(1,1)} = \int d\xi\{\hat{m}\cdot\hat{m}\cdot\hat{m}\cdot\hat{m}\cdot\tau_Z\cdot\hat{m}\}_{(1,1)} = \frac{5i}{8}\frac{\pi\Delta^2\omega_n\hbar^6}{(\Delta^2+(\hbar\omega_n)^2)^{7/2}},$$

$$\hat{\tau}_Z\hat{\tau}_Z: -\int d\xi\{\hat{m}\cdot\tau_Z\cdot\hat{m}\cdot\hat{\tau}_Z\cdot\hat{m}\cdot\hat{m}\}_{(1,1)} = -\int d\xi\{\hat{m}\cdot\hat{m}\cdot\hat{\tau}_Z\cdot\hat{m}\cdot\tau_Z\cdot\hat{m}\}_{(1,1)} = \frac{1}{2}\int d\xi\{\hat{m}\cdot\hat{\tau}_Z\cdot\hat{m}\cdot\hat{m}\cdot\tau_Z\cdot\hat{m}\}_{(1,1)} = \frac{1}{4}\frac{\pi\Delta^2\hbar^4}{(\Delta^2+(\hbar\omega_n)^2)^{5/2}}. \quad \text{(B5)}$$

It follows that the sum of the four terms involving one $\hat{\tau}_Z$ matrix factor and the sum of the three terms involving two $\hat{\tau}_Z$ factors in (B5) are exactly zero. This result shows that unlike the situation in the third order, the fifth order in each of the $(\vec{A}\cdot\vec{A})$ terms does not vanish, yet their sum cancels out exactly.

In the seventh order there are 20 terms involving the $(\vec{A}\cdot\vec{A})$ interaction of the type (B5). These are easily classified into groups of six, ten, and four terms associated with one, two, and three $\hat{\tau}_Z$ matrix factors, respectively. As in Eq. (B4), these terms do not vanish individually; however, their sums within each class defined by a fixed number of $\hat{\tau}_Z$ factors cancel out exactly. The same situation recurs in the ninth order. In this case there are 54 terms, classified into groups according to the number of $\hat{\tau}_Z$ factors in each integrand (four $\hat{\tau}_Z$ factors at the most). A lengthy explicit calculation shows that as in Eq. (B5), the sums of terms within each class cancel exactly. The emerging pattern from these results is that all $(\vec{A}\cdot\vec{A})$ terms in all odd-order terms (in $\vec{A}$) in expansion (2.2) can be discarded.

APPENDIX C: DECOUPLING OF INTEGRATIONS IN THE FIFTH-ORDER TERM IN EQ. (2.7)

The arguments and steps below follow those applied to the third-order term in Eq. (2.7) in Ref. 5, where the q and $\vec{k}_1$ integrations are approximately decoupled. By extension, the same applies to all higher-order terms in the CR expansion.

In Eq. (2.7) the k_1 variable is associated with the Green function factors $\hat{G}_0$, and the q variables are associated with the $\vec{A}$ factors. The Green function $\hat{G}_0(\vec{k},\omega_n)$ draws its main contribution from momenta near the Fermi surface, i.e., $|\vec{k}| \sim k_f$,[6] while the self-consistent vector potential $\vec{A}(\vec{q})$, approximately a Lorentzian, is significant only for momenta in the range $0<q\leqslant\lambda^{-1}\ll k_F$.[9] Consequently, all q_i-momenta dependencies in the $\hat{G}_0$ factors are neglected. The remaining q_i integrations are constrained only by the scalar-product factors in Eq. (2.7). The product of these scalar-product factors presumably attain a maximum at particular points in the q_i-momenta space, with a characteristic falloff over a length scale on the order of λ_0^{-1}. These maxima occur when the q_i momenta are such that all scalar-product factors in Eq. (2.7) attain their maximum.

Note that by $\vec{A}\|\vec{B}$ parallelism of two vectors $\vec{A}$ and $\vec{B}$, all fifth-order term scalar products simultaneously attain their maximum when

$$\begin{aligned}
&(1)\ \vec{A}(\vec{q}_1)\|\vec{k}_1,\\
&(2)\ \vec{A}(\vec{q}_2)\|\vec{k}_1-\vec{q}_1,\\
&(3)\ \vec{A}(\vec{q}_3)\|\vec{k}_1-\vec{q}_1-\vec{q}_2,\\
&(4)\ \vec{A}(\vec{q}_4)\|\vec{k}_1-\vec{q}_1-\vec{q}_2-\vec{q}_3,\\
&(5)\ \vec{A}(\vec{q}-\vec{q}_1-\vec{q}_2-\vec{q}_3-\vec{q}_4)\|\vec{k}_1-\vec{q},
\end{aligned}\tag{C1}$$

To identify the $\vec{q}_i$ momenta where all (C1) conditions are satisfied, first compare conditions (4) and (5). Their right-hand sides coincide provided $\vec{q}=\vec{q}_1+\vec{q}_2+\vec{q}_3$. Inserting the latter momenta equation and noting that the chosen gauge $(\vec{k}\cdot\vec{A}(\vec{k}))=0$, it follows that conditions (3)–(5) in (C1) are transformed into

$$\begin{aligned}
&(3')\ \vec{A}(\vec{q}_3)\|\vec{k}_1-\vec{q},\\
&(4')\ \vec{A}(\vec{q}_4)\|\vec{k}_1-\vec{q},\\
&(5')\ \vec{A}(-\vec{q}_4)\|\vec{k}_1-\vec{q}.
\end{aligned}\tag{C2}$$

Conditions (4′) and (5′) in Eq. (C2) are consistent noting that the vector potential, by assumption (Fig. 1), is aligned in the $\hat{x}$ direction. These conditions coalesce provided $\vec{q}_3=\pm\vec{q}_4$.

Condition (2) in Eq. (C1) can be added to the set of maximum-value scalar products (C2) provided $\vec{q}_1=\vec{q}$, $\vec{q}_2=\pm\vec{q}_3=\pm\vec{q}_4$. However, in order to satisfy the constraint $\vec{q}=\vec{q}_1+\vec{q}_2+\vec{q}_3$ it follows that $\vec{q}_2=-\vec{q}_3=\pm\vec{q}_4$. Next, using the gauge condition $(\vec{k}\cdot\vec{A}(\vec{k}))=0$, condition (1) in Eq. (C1) takes the form $\vec{A}(\vec{q})\|\vec{k}_1-\vec{q}$. Comparing the latter with Eq. (C2) yields $\pm\vec{q}_4=\vec{q}$. These considerations imply that the locus in the $\{q_1,q_2,q_3,q_4\}$ space where all conditions Eq. (C1) coalesce are the points where $|q_i|=|q|$. In the long-wavelength limit, to which all subsequent discussion is limited, these maxima points coalesce into one point.

To examine the integrand's falloff around the maxima points in the q_i-momenta space, we introduce auxiliary momenta variables κ_i to denote the deviation from a maximum point. Two plausible analytic form factors are postulated for the falloff. Both form factors, i.e., a Gaussain and a Lorenztian form factor, share the same maximum value and falloff range λ_0; they differ, however, in the falloff rapidity. Explicitly, consider

$$\mathbb{R}(\kappa)=\frac{(\vec{A}(q+\kappa)\cdot\vec{k}_1)}{(\vec{A}(q)\cdot\vec{k}_1)}=\begin{cases} e^{-(\kappa^*\lambda_0)^2} \\ 1/(1+(\kappa^*\lambda_0)^2)\end{cases}.\tag{C3}$$

In terms of the κ_i variables, the q_i integrations associated with the third- and fifth-order terms in Eq. (2.7) take the form

$$\int_{-\infty}^{\infty}d\kappa_1\int_{-\infty}^{\infty}d\kappa_2\mathbb{R}(\kappa_1)\mathbb{R}(\kappa_1)\mathbb{R}(q-\kappa_1-\kappa_2)=\frac{\alpha^{(3)}(q\lambda_0)}{\lambda_0^2},$$

$$\int_{-\infty}^{\infty}d\kappa_1\int_{-\infty}^{\infty}d\kappa_2\int_{-\infty}^{\infty}d\kappa_3\int_{-\infty}^{\infty}d\kappa_4\mathbb{R}(\kappa_1)\mathbb{R}(\kappa_2)\mathbb{R}(\kappa_3)\mathbb{R}(\kappa_4)$$
$$\times\mathbb{R}(q-\kappa_1-\kappa_2-\kappa_3-\kappa_4)=\frac{\alpha^{(5)}(q\lambda_0)}{\lambda_0^4}.\tag{C4}$$

The structure of the terms in Eq. (C4) indicates that of the corresponding integrals associated with the higher-order terms in Eq. (2.7). Fortunately, these integrals are available analytically. Employing the notation in Eq. (C4) with self-evident generalizations the results for the lowest orders are

n	$\alpha^{(n)}((q\lambda_0)$;Lorentzian)	$\alpha^{(n)}((q\lambda_0)$;Gaussian)
3	$\frac{3\pi^2}{9+(q\lambda_0)^2}$	$\frac{\pi e^{-(q\lambda_0)^2/3}}{\sqrt{3}}$
5	$\frac{5\pi^4}{25+(q\lambda_0)^2}$	$\frac{\pi^2 e^{-(q\lambda_0)^2/5}}{\sqrt{5}}$
7	$\frac{7\pi^6}{49+(q\lambda_0)^2}$	$\frac{\pi^3 e^{-(q\lambda_0)^2/7}}{\sqrt{7}}$
9	$\frac{9\pi^8}{81+(q\lambda_0)^2}$	$\frac{\pi^4 e^{-(q\lambda_0)^2/9}}{\sqrt{9}}$.

(C5)

Accordingly, the decoupled q_i integrations in the third- and fifth-order terms in Eq. (2.7) are

$$\int dq_1 dq_2 (\vec{A}(\vec{q}_1)\cdot\vec{k}_1)(\vec{A}(\vec{q}_2)\cdot\vec{k}_1-\vec{q}_1)(\vec{A}(\vec{q}-\vec{q}_1-\vec{q}_2)\cdot\vec{k}_1-\vec{q}_1)$$
$$\approx \frac{\alpha^{(3)}(q\lambda_0)}{\lambda_0^2}(\vec{A}(\vec{q})\cdot\vec{k}_1)^2(\vec{A}(-\vec{q})\cdot\vec{k}_1),$$

$$\int dq_1 dq_2 dq_3 dq_4 (\vec{A}(\vec{q}_1)\cdot\vec{k}_1)(\vec{A}(\vec{q}_2)\cdot(\vec{k}_1-\vec{q}_1))$$
$$\times(\vec{A}(\vec{q}_3)\cdot(\vec{k}_1-\vec{q}_1-\vec{q}_2))\times(\vec{A}(\vec{q}_4)\cdot(\vec{k}_1-\vec{q}_1-\vec{q}_2-\vec{q}_3))$$
$$\times(\vec{A}(\vec{q}-\vec{q}_1-\vec{q}_2-\vec{q}_3-\vec{q}_4)\cdot(\vec{k}_1-\vec{q}))$$
$$\approx \frac{\alpha^{(5)}(q\lambda_0)}{\lambda_0^4}(\vec{A}(\vec{q})\cdot\vec{k}_1)^3(\vec{A}(-\vec{q})\cdot\vec{k}_1)^2. \quad \text{(C6)}$$

APPENDIX D: EVALUATION OF THE INTEGRATION AND SUMMATION IN EQ. (2.9) FOR A *d*-WAVE GAP FUNCTION

In the context of HTS and its presumed cylindrical Fermi surface,[5] the cylindrical coordinate system is the coordinate system of choice. In terms of the Cartesian coordinate system in Fig. 1, both systems are related by

$$\vec{k}_1 = \hat{x}K\cos\theta + \hat{y}K\sin\theta + \hat{z}k_z,$$

$$\vec{A}(\vec{q}) = \hat{x}A(q) = \vec{A}^*(-\vec{q}), \quad (\vec{A}(q)\cdot\vec{k}) = A(q)K\cos\theta. \quad \text{(D1)}$$

Consequently, the momentum integration and summation in Eq. (2.9) takes the form

$$\int d\vec{k}_1 \vec{k}_1 (\vec{A}(\vec{q})\cdot\vec{k}_1)^2(\vec{A}(-\vec{q})\cdot\vec{k}_1)\{\cdots\}_{(1,1)}$$
$$= \int_0^\infty dK K^5 \int_{-\infty}^\infty dk_z A(q)|A(q)|^2 \int_0^{2\pi} d\theta \cos^3$$
$$\times\theta\left(\hat{x}\cos\theta+\hat{y}\sin\theta+\hat{z}\frac{k_z}{K}\right)\{\cdots\}_{(1,1)},$$

$$\{\cdots\}_{(1,1)} = \left\{\hat{G}_0^4(\vec{k}_1;\omega_n)\times\left(\vec{I}+\left(\frac{3}{5}\right)(\varepsilon(K)\cos^2\theta)\hat{G}_0^2(\vec{k}_1;\omega_n)\right.\right.$$
$$+\left(\frac{3}{7}\right)(\varepsilon(K)\cos^2\theta)^2\hat{G}_0^4(\vec{k}_1;\omega_n)+\left(\frac{3}{9}\right)$$
$$\left.\left.\times(\varepsilon(K)\cos^2\theta)^4\hat{G}_0^6(\vec{k}_1;\omega_n)+\cdots\right)\right\}_{(1,1)}, \quad \text{(D2)}$$

where we introduced an interim, momentum-dependent expansion parameter ε,

$$\varepsilon(K) = \left(\frac{q_S}{2mc\lambda_0}\right)^2 |A(q)|^2 K^2. \quad \text{(D3)}$$

The assumed gap function is the standard $d_{x^2-y^2}$ d-wave symmetry gap function.[10] Its Fourier transform in the relative-momentum space (Appendix A) is

$$\Delta(\vec{k};T) = \Delta(\theta;T) = \Delta_0(T)\cos(2\theta). \quad \text{(D4)}$$

The triple integration in (D2) is now reduced to a double integration following the standard observation that the Green function draws most of its strength near the Fermi surface,[6] and $m_{ab} \ll m_c$.[11] Noting these simplifying factors, the K-momentum integration in (D2) is replaced by integration over the relative energy ξ,[5] where

$$\xi(K,k_z) = \frac{\hbar^2K^2}{2m_{ab}} + \frac{\hbar^2k_z}{2m_z} - \mu \approx \frac{\hbar^2K^2}{2m_{ab}} - \mu = \xi(K). \quad \text{(D5)}$$

A similar argument implies that the k_z integration runs along the height of the Fermi-cylinder surface. Combining these steps yields for the momenta integrations in (D2),

$$\int_{-\infty}^\infty dk_z \int_0^\infty dK K^5 F(K,k_z,\theta)$$
$$\approx 8k_F(\hat{c})\left(\frac{m_{ab}}{\hbar^2}\right)^3\mu^2\int_{-\infty}^\infty d\xi F(K(\xi),\theta). \quad \text{(D6)}$$

In (D6) the symbol F denotes the integrand in (D2), and we used from (D5) and the above

$$K \approx \sqrt{\frac{2m_{ab}\mu}{\hbar^2}}, \quad \int_{-\infty}^\infty dk_z \approx 2k_F(\hat{c}) \approx \frac{2\pi}{a_c}. \quad \text{(D7)}$$

Regarding the angular integrations in (D2), noting the dependence of the gap function (D4) on $\cos(2\theta)$, and given the angular integrals

$$\int_0^{2\pi} d\theta(\cos\theta)^3(\cos(2\theta))^n = 0,$$
$$\int_0^{2\pi} d\theta(\cos\theta)^3\sin(\theta)(\cos(2\theta))^n = 0, \quad \text{(D8)}$$

it follows that only the $\hat{x}$ component survives the angular integrations in (D2). These steps together yield the following expression for the nonlinear current Eq. (2.9):

$$\vec{j}_{\mathrm{NL}}(q) \approx -\frac{2q_S^4\alpha^{(3)}(q)}{\beta(2\pi)^5 m^4 c^3 {\lambda_0}^2}\sum_{n=-\infty}^{\infty}\int d\vec{k}_1\vec{k}_1(\vec{A}(\vec{q})\cdot\vec{k}_1)^2(\vec{A}(-\vec{q})\cdot\vec{k}_1)\{\cdots\}_{(1,1)}$$

$$= -\vec{A}(q)\frac{16q_S^4\alpha^{(3)}(0)k_F(\hat{c})\mu^2|A(q)|^2}{m\beta(2\pi)^5c^3{\lambda_0}^2\hbar^6}\sum_{n=-\infty}^{\infty}\int_0^{2\pi}d\theta\cos^4\theta\int_{-\infty}^{\infty}d\xi\Bigg\{\hat{G}_0^4(\xi;\omega_n)\times\left(\overleftrightarrow{I}+\left(\frac{3}{5}\right)(v\cos^2\theta)\left(\left(\frac{\Delta_0}{\hbar}\right)\hat{G}_0(\vec{k}_1;\omega_n)\right)^2+\left(\frac{3}{7}\right)\right.$$

$$\left.\times(v\cos^2\theta)^2\left(\left(\frac{\Delta_0}{\hbar}\right)\hat{G}_0(\vec{k}_1;\omega_n)\right)^4+\left(\frac{3}{9}\right)(v\cos^2\theta)^3\left(\left(\frac{\Delta_0}{\hbar}\right)\hat{G}_0(\vec{k}_1;\omega_n)\right)^6+\cdots\right)\Bigg\}_{(1,1)}, \tag{D9}$$

where the dimensionless, angle-independent expansion parameter v [Eq. (2.13)] is

$$v = \frac{q_S^2\mu|A(q)|^2}{2mc^2{\lambda_0}^2\Delta_0^2}. \tag{D10}$$

The remaining nontrivial challenge of expression (D9) is performing the matrix series summation in the integrand. For this purpose recast the sum in the form

$$\mathbb{Z}(\omega) = \left\{\hat{G}_0^4(\omega)\sum_{n=0}^{\infty}\frac{3}{2n+3}(\gamma\hat{G}_0^2(\omega))^n\right\}_{(1,1)},$$

$$\gamma = v\left(\frac{\Delta_0}{\hbar}\right)^2\cos^2\theta, \tag{D11}$$

where the Green function matrix $\hat{G}_0$ is given in Ref. 5. The summation in (D11) can be carried out exactly. The result simplifies considerably provided all odd ξ-power terms are dropped, noting that they will not contribute due to the ξ integration in Eq. (D9) in any case. These steps yield for the series (D11),

$$\mathbb{Z}(\omega)|_{\text{Even Powers in }\xi} = -\frac{3\hbar^2(\xi^2+\Delta^2-\hbar^2\omega^2)}{\gamma(\xi^2+\Delta^2+\hbar^2\omega^2)}+\left(\frac{3\hbar}{2\gamma^{3/2}}\right)\times\left(\left(\frac{1}{(\sqrt{\xi^2+\Delta^2}-i\hbar\omega)}\right)\times\operatorname{arctanh}\left(\frac{\hbar\sqrt{\gamma}}{\sqrt{\Delta^2}-i\hbar\omega}\right)+\text{c.c.}\right). \tag{D12}$$

Note that $\mathbb{Z}(\omega)$ entails an angular dependence, which resides in the gap function Δ, Eq. (D4), and in the modified expansion parameter γ, Eq. (D11).

To gain confidence with expression (D12), it can be checked against the simpler, geometric matrix series

$$\mathbb{C}(\omega) = \left\{\hat{G}_0^4(\omega)\times\sum_{n=0}^{\infty}(\gamma\hat{G}_0^2(\omega))^n\right\}_{(1,1)}$$

$$= \{\hat{G}_0^4(\omega)\times(\overleftrightarrow{I}-\gamma\hat{G}_0^2(\omega))^{-1}\}_{(1,1)}. \tag{D13}$$

The series $\mathbb{C}(\omega)$ is considerably simpler to evaluate, with the result

$$\mathbb{C}(\omega)|_{\text{Even Powers in }\xi} = \frac{\hbar^4((\xi^2+\Delta^2)^2-\hbar^2(\xi^2+\Delta^2)(\gamma+6\omega^2)+\hbar^4\omega^2(\gamma+\omega^2))}{(\xi^2+\Delta^2+\hbar^2\omega^2)^2((\xi^2+\Delta^2)^2-2\hbar^2(\xi^2+\Delta^2)(\gamma-\omega^2)+\hbar^4(\gamma+\omega^2)^2)}. \tag{D14}$$

One check of Eq. (D12) is to examine its expansion in powers of γ against the corresponding expansion of Eq. (D14), and verify that the coefficients match, except for the different weights of $(3/5),(3/7),(3/9),\ldots$ in Eq. (D11). The expansion of Eq. (D12) to second order in γ is

$$\mathbb{Z}(\omega)|_{\text{Even Powers in }\xi} = \frac{\hbar^4(\xi^4+\Delta^4-6\Delta^2\hbar^2\omega^2+\hbar^4\omega^4+2\xi^2(\Delta^2-3\hbar^2\omega^2))}{(\xi^2+\Delta^2+\hbar^2\omega^2)^4}+3\hbar^6[\xi^6+3\xi^4(\Delta^2-5\hbar^2\omega^2)+3\xi^2(\Delta^4-10\Delta^2\hbar^2\omega^2$$

$$+5\hbar^4\omega^4)+\Delta^6-15\Delta^4\hbar^2\omega^2+15\Delta^2\hbar^4\omega^4-\hbar^6\omega^6]\left(\frac{1}{5(\xi^2+\Delta^2+\hbar^2\omega^2)^6}\right)\gamma+O(\gamma^2). \tag{D15}$$

When (D15) is compared to the corresponding expansion of Eq. (D14) to second order in γ (not shown), the terms match except for the different weights in (D11).

The remaining two integrations in expression (D9) cannot be carried out analytically. However, in the geometrical-series approximation, Eqs. (D13) and (D14), the ξ integration

can be done analytically with the result

$$\mathbb{Q}(\theta,\omega_n) = \int_{-\infty}^{\infty} d\xi(\hat{G}_0^4(\xi,\theta;\omega_n)(\overleftrightarrow{I} - \gamma\hat{G}_0^2(\xi,\theta;\omega_n))^{-1})_{(1,1)}$$
$$= \frac{\pi\hbar^2}{2\gamma}\left(\frac{\sqrt{\gamma}-i\omega_n}{\sqrt{\gamma}\sqrt{\Delta^2-\hbar^2(\sqrt{\gamma}-i\omega_n)^2}}\right.$$
$$\left. + \frac{\sqrt{\gamma}+i\omega_n}{\sqrt{\gamma}\sqrt{\Delta^2-\hbar^2(\sqrt{\gamma}+i\omega_n)^2}} - \frac{2\Delta^2}{(\Delta^2+(\hbar\omega_n)^2)^{3/2}}\right). \tag{D16}$$

The expansion of Eq. (D16) to the two lowest orders of γ is

$$\mathbb{Q}(\theta,\omega_n) = \frac{\pi\hbar^4(\Delta^4-4(\hbar\omega_n)^2\Delta^2)}{2(\Delta^2+(\hbar\omega_n)^2)^{7/2}}$$
$$+ \frac{3\pi\hbar^6(\Delta^6-12\Delta^4(\hbar\omega_n)^2+8\Delta^2(\hbar\omega_n)^4)\gamma}{8(\Delta^2+(\hbar\omega_n)^2)^{11/2}} + O(\gamma^2). \tag{D17}$$

The first term on the right-hand side of Eq. (D17) is precisely the expression obtained in Ref. 5 for the third-order CR. The next-order term in Eq. (D17) has been verified by explicitly evaluating the $\hat{G}_0^6$ term in the expansion of Eq. (D13).

[1] D. E. Oates, S.-H. Park, D. Agassi, and G. Koren, Supercond. Sci. Technol. **17**, S290 (2004), and references therein.

[2] D. E. Oates, S.-H. Park, and G. Koren, Phys. Rev. Lett. **93**, 197001 (2004); D. E. Oates, S.-H. Park, D. Agassi, G. Koren, and K. Irgmaier, IEEE Trans. Appl. Supercond. **15**, 3589 (2005).

[3] S. K. Yip and J. A. Sauls, Phys. Rev. Lett. **69**, 2264 (1992); D. Xu, S. K. Yip, and J. A. Sauls, Phys. Rev. B **51**, 16233 (1995).

[4] T. Dahm, D. J. Scalapino, and B. A. Willemsen, J. Supercond. **12**, 339 (1999); T. Dahm and D. J. Scalapino, Phys. Rev. B **60**, 13125 (1999); Appl. Phys. Lett. **81**, 2002 (1997).

[5] D. Agassi and D. E. Oates, Phys. Rev. B **72**, 014538 (2005).

[6] A. L. Fetter and J. D. Walecka, *Quantum Theory of Many Particle Systems* (McGraw-Hill, New York, 1971).

[7] M. E. Flatte and J. M. Byers, in *Solid State Physics*, edited by H. Ehrenreich and F. Spaepen (Academic, San Diego, 1999), Vol. 52, p. 138.

[8] A. Abrikosov, L. Gorkov, and I. Dzyaloshinski, *Methods of Quantum Field Theory in Statistical Physics* (Dover, New York, 1963), Sect. 39; D. Agassi and D. E. Oates, J. Supercond. **16**, 905 (2003).

[9] M. Tinkham, *Introduction to Superconductivity*, 2nd ed. (McGraw-Hill, New York, 1996).

[10] See, e.g., J. Y. T. Wei, N. C. Yeh, D. F. Garrigus, and M. Strasik, Phys. Rev. Lett. **81**, 2542 (1998).

[11] C. P. Poole, A. A. Farach, and R. J. Creswick, *Superconductivity* (Academic, San Diego, 1995), pp. 502, 543; P. B. Allen, W. E. Pickett, and H. Krakauer, Phys. Rev. B **37**, 7482 (1988); P. B. Allen, W. E. Pickett, and H. Krakauer, *ibid.* **36**, 3926 (1987); R. T. Collins, Z. Schlesinger, F. H. Holtzberg, P. Chaudhari, and C. A. Feild, IBM J. Res. Dev. **33**, 238 (1989).

[12] D. M. Sheen, S. M. Ali, D. E. Oates, R. S. Withers, and J. A. Kong, IEEE Trans. Appl. Supercond. **1**, 108 (1991).

[13] J. G. Ossandon, J. R. Thompson, D. K. Christen, B. C. Sales, H. R. Kerchner, J. O. Thomson, Y. R. Sun, K. W. Lay, and J. E. Tkaczyk, Phys. Rev. B **45**, 12534 (1992); D. Agassi and J. R. Cullen, Physica C **334**, 259 (2000).

[14] T. Van Duzer and C. W. Turner, *Principles of Superconductive Devices and Circuits* (Elsevier, New York, 1981), Sec. 3.15.

[15] D. Agassi and J. R. Cullen, Physica C **195**, 277 (1992).

[16] See, e. g., D. Agassi, D. K. Christen, and S. J. Pennycook, Appl. Phys. Lett. **81**, 2803 (2002); D. Agassi, C. S. Pande, and R. A. Masumura, Phys. Rev. B **52**, 16237 (1995); I. Maggio-April, C. Renner, A. Erb, E. Walker, and O. Fischer, Nature (London) **390**, 487 (1997).

[17] In Ref. 9, p. 346.

[18] N. Belk, D. E. Oates, D. A. Feld, G. Dresselhaus, and M. S. Dresselhaus, Phys. Rev. B **53**, 3459 (1996).

[19] M. W. Coffey and J. R. Clem, Phys. Rev. B **48**, 342 (1993); M. Benkraouda and J. R. Clem, *ibid.* **53**, 5716 (1996); J. McDonald, J. R. Clem, and D. E. Oates, *ibid.* **55**, 11823 (1997).

[20] Y. M. Habib, C. J. Lehner, D. E. Oates, L. R. Vale, R. H. Ono, G. Dresselhaus, and M. S. Dresselhaus, Phys. Rev. B **57**, 13833 (1998), and references therein.

[21] N. Belk, D. E. Oates, D. A. Feld, G. Dresselhaus, and M. S. Dresselhaus, Phys. Rev. B **56**, 11966 (1997); J. R. Powell, A. Porch, R. G. Humphreys, F. Wellhofer, M. J. Lancaster, and C. E. Gough, *ibid.* **57**, 5474 (1998).

[22] In Ref. 6, p. 444.

[23] J. R. Schrieffer, *Theory of Superconductivity* (Benjamin, New York, 1964), pp. 12–13, and Sec. (8.5).

[24] In Ref. 5, Eq. (A5) there is a misprint. It should read $\vec{q} = (0,0,q_Z)$.

[25] E. J. Nicol and J. P. Carbotte, Phys. Rev. B **73**, 174510 (2006); E. J. Nicol, J. P. Carbotte, and D. J. Scalapino, *ibid.* **73**, 014521 (2006).

[26] Y. Ren, J. H. Xu, and C. S. Ting, Phys. Rev. Lett. **74**, 3680 (1995).